

BO 2.0: Plasma Wave and Instability Analysis with Enhanced Polarization Calculations

Hua-sheng XIE^{a,b}, Richard Denton^c, Jin-song Zhao^{d,e}, Wen Liu^{d,e}

^aHebei Key Laboratory of Compact Fusion, Langfang 065001, China

^bENN Science and Technology Development Co., Ltd., Langfang 065001, China

^cDepartment of Physics and Astronomy, Dartmouth College, Hanover, New Hampshire, USA

^dKey Laboratory of Planetary Sciences, Purple Mountain Observatory, Chinese Academy of Sciences, Nanjing 210008, People's Republic of China

^eSchool of Astronomy and Space Science, University of Science and Technology of China, Hefei 230026, People's Republic of China

Abstract

Besides the relation between the wave vector \mathbf{k} and the complex frequency ω , wave polarization is useful for characterizing the properties of a plasma wave. The polarization of the electromagnetic fields, $\delta\mathbf{E}$ and $\delta\mathbf{B}$, have been widely used in plasma physics research. Here, we derive equations for the density and velocity perturbations, δn_s and $\delta \mathbf{v}_s$, respectively, of each species in the electromagnetic kinetic plasma dispersion relation by using their relation to the species current density perturbation $\delta \mathbf{J}_s$. Then we compare results with those of another commonly used plasma dispersion code (WHAMP) and with those of a multi-fluid plasma dispersion relation. We also summarize a number of useful polarization quantities, such as magnetic ellipticity, orientation of the major axis of the magnetic ellipse, various ratios of field energies and kinetic energies, species compressibility, parallel phase ratio, Alfvén-ratio, etc., which are useful for plasma physics research, especially for space plasma studies. This work represents an extension of the BO electromagnetic dispersion code [H.S. Xie, *Comput. Phys. Comm.* 244 (2019) 343-371] to enhance its calculation of polarization and to include the capability of solving the electromagnetic magnetized multi-fluid plasma dispersion relation.

Keywords: Plasma physics, Kinetic dispersion relation, Waves and instabilities, Matrix eigenvalue

PROGRAM SUMMARY

Program Title: BO 2.0

Licensing provisions: BSD 3-clause

Programming language: Matlab

Journal reference of previous version: [1] H.S. Xie, BO: A unified tool for plasma waves and instabilities analysis, *Comput. Phys. Comm.* 244 (2019) 343-371. [2] H.S. Xie, Y. Xiao, PDRK: A General Kinetic Dispersion Relation Solver for Magnetized Plasma, *Plasma Sci. Technol.* 18 (2) (2016) 97. [3] H. S. Xie, PDRF: A general dispersion relation solver for magnetized multi-fluid plasma, *Comput. Phys. Comm.* 185 (2014) 670-675.

Does the new version supersede the previous version?: Yes

Reasons for the new version: Enhance the code capability, especially to support the calculation of density and velocity perturbations. Also, the multi-fluid and kinetic versions are combined into one version.

*Summary of revisions:** In this new version, multi-fluid model is included as one option. The density and velocity perturbations of kinetic versions are also supported. Many useful polarizations are included.

Nature of problem: The linear fluid and kinetic waves and instabilities in plasma can be described by dispersion relations. The challenges are to provide a dispersion relation as general as possible and to obtain all the solutions of it, which is the goal of BO. The BO code provides a unified numerically solvable framework for kinetic and multi-fluid plasma dispersion relations, which greatly extends the standard ones, with an arbitrary number of species.

Solution method: Transforming the dispersion relation to an equivalent matrix eigenvalue problem and find all the solutions using standard matrix eigenvalue library function.

Email addresses: huashengxie@gmail.com, xiehuasheng@enn.cn (Hua-sheng XIE), redenton@gmail.com (Richard Denton), js_zhao@pmo.ac.cn (Jin-song Zhao)

Additional comments including Restrictions and Unusual features (approx. 50-250 words): Kinetic relativistic effects are not included in the present version yet.

1. Introduction

Plasma is a combination of particles and electromagnetic fields. The electromagnetic fields are usually described by the Maxwell equations, whereas particles can be described by either a kinetic model using the distribution function, $f_s(\mathbf{v}, t)$, or a fluid model that employs velocity moments of the distribution function. It is well known that, for a uniform plasma, the linear plasma dispersion relation can be solved using

$$\mathbf{D} \cdot \delta\mathbf{E} = 0, \quad (1)$$

with

$$|D(\omega, \mathbf{k})| = 0, \quad (2)$$

where \mathbf{D} is a 3-by-3 matrix tensor and $\delta\mathbf{E} = (\delta E_x, \delta E_y, \delta E_z)$ is the perturbed electric field. For a given wave vector \mathbf{k} , we solve the dispersion relation Eq.(2), which yields the complex frequency, $\omega = \omega_r + i\omega_i$. Then, we obtain the matrix elements of \mathbf{D} from ω and solve Eq. (1) for the perturbed electric field $\delta\mathbf{E}$. We can then calculate the perturbed magnetic field $\delta\mathbf{B}$ and current density $\delta\mathbf{J}$ using the Maxwell equations.

Besides the perturbed electromagnetic fields, the plasma waves can carry the perturbed density δn_s and velocity $\delta\mathbf{v}_s$, which are widely used for the wave mode identification. Here ‘‘s’’ denotes the particle species. δn_s and $\delta\mathbf{v}_s$ were not given in the kinetic dispersion code BO v1.0 [1, 2], which has been shown to be a powerful tool for studying plasma waves and instabilities in the solar-terrestrial plasmas [4, 5]. The major purpose of this work is to derive expressions for δn_s and $\delta\mathbf{v}_s$ using the kinetic dispersion relation, and check the validity of the approach by comparing results with those of another commonly used electromagnetic dispersion code (WHAMP [6]) and with those of a multi-fluid plasma model [3]. In section 2, we derive the equations and show how we implement them in the BO kinetic dispersion code [1, 2] and the PDRK fluid dispersion code [3]. In section 3, we benchmark the results using two independent kinetic solvers and with the multi-fluid solver PDRF. In section 4, we give a summary with some discussion. In the Appendices, we list useful polarization quantities calculated in BO and give a summary of the updated model used in PDRF. All of these updates are summarized to the new version BO v2.0 (<https://github.com/hsxie/bo>).

2. How to calculate the perturbed density, velocity and plasma current in BO

2.1. Perturbed density and velocity

In the plasma kinetic model, the density and velocity are zeroth and first order moment of the velocity distribution function, respectively. The perturbed density is given by $\delta n_s = n_{s0} \int \delta f_s d\mathbf{v}^3$, where n_{s0} is the zeroth order density and δf_s is the first order perturbed velocity distribution function. The controlling equation for the perturbed density can be obtained through performing zeroth order moment for the linear Vlasov equation,

$$\partial_t \delta n_s + \nabla \cdot (\delta\mathbf{J}_s / q_s) = 0, \quad (3)$$

where $\delta\mathbf{J}_s = n_{s0} q_s \int \mathbf{v} \delta f_s d\mathbf{v}^3$ is the perturbed plasma current. The perturbed plasma current can be expressed in terms of the perturbed fluid density and velocity,

$$\delta\mathbf{J}_s = q_s n_{s0} \delta\mathbf{v}_s + q_s \delta n_s \mathbf{v}_{ds}, \quad (4)$$

or

$$\begin{cases} \delta J_{sx} &= q_s n_{s0} \delta v_{sx} + q_s \delta n_s v_{dsx}, \\ \delta J_{sy} &= q_s n_{s0} \delta v_{sy} + q_s \delta n_s v_{dsy}, \\ \delta J_{sz} &= q_s n_{s0} \delta v_{sz} + q_s \delta n_s v_{dsz}, \end{cases} \quad (5)$$

where $\mathbf{v}_{ds} = (v_{dsx}, v_{dsy}, v_{dsz})$ denotes the zeroth order drift velocity, and directions of x and y axes are perpendicular to the background magnetic field $\mathbf{B}_0 = B_0\mathbf{z}$. It should be noted that one of advantages of BO [1] and PDRF [3] is that the three components of \mathbf{v}_{ds} are included in these two solvers.

Using Eqs. (3) and (5), we can directly obtain δn_s and $\delta \mathbf{v}_s$, once the dispersion relation of one plasma wave mode and $\delta \mathbf{J}_s$ are known. Under the plane wave assumption, i.e., $\partial_t \rightarrow -i\omega$, $\nabla \rightarrow i\mathbf{k}$, one readily obtains

$$\omega \delta n_s = \frac{1}{q_s} \mathbf{k} \cdot \delta \mathbf{J}_s. \quad (6)$$

Since the wavevector is given as $\mathbf{k} = (k_x, 0, k_z)$ in BO [1], the controlling equations for the perturbed density and velocity are

$$\begin{cases} \delta n_s &= \frac{1}{\omega q_s} (k_x \delta J_{sx} + k_z \delta J_{sz}), \\ \delta v_{sx} &= \frac{1}{q_s n_{s0}} \left[\delta J_{sx} - \frac{1}{\omega} (k_x \delta J_{sx} + k_z \delta J_{sz}) v_{dsx} \right], \\ \delta v_{sy} &= \frac{1}{q_s n_{s0}} \left[\delta J_{sy} - \frac{1}{\omega} (k_x \delta J_{sx} + k_z \delta J_{sz}) v_{dsy} \right], \\ \delta v_{sz} &= \frac{1}{q_s n_{s0}} \left[\delta J_{sz} - \frac{1}{\omega} (k_x \delta J_{sx} + k_z \delta J_{sz}) v_{dsz} \right]. \end{cases} \quad (7)$$

Here we note that $\delta \mathbf{v}_s = \int d\mathbf{v}^3 \mathbf{v} \delta f_s = \delta \mathbf{J}_s / n_{s0} / q_s$ in motionless plasmas where $\mathbf{v}_{ds} = 0$, and $\delta \mathbf{v}_s \neq \int d\mathbf{v}^3 \mathbf{v} \delta f_s$ in a plasma where $\mathbf{v}_{ds} \neq 0$.

2.2. Perturbed plasma current

In this subsection, we will discuss how to calculate the plasma current $\delta \mathbf{J}_s$ in BO/PDRK [1, 2]. The first approach for giving $\delta \mathbf{J}_s$ is through $\delta \mathbf{J}_s = \boldsymbol{\sigma}_s \cdot \delta \mathbf{E}$, where the conductivity tensor $\boldsymbol{\sigma}_s$ in BO/PDRK can be obtained by the following procedures. Eq. (129) in Ref. [1] gives the relation of the total plasma current and electric field in BO/PDRK

$$\begin{pmatrix} \delta J_x^m \\ \delta J_y^m \\ \delta J_z^m \end{pmatrix} = -i\epsilon_0 \begin{pmatrix} \frac{b_{11}^m}{\omega} + \sum_{snj} \frac{b_{snj11}}{\omega - c_{snj}} & \frac{b_{12}^m}{\omega} + \sum_{snj} \frac{b_{snj12}}{\omega - c_{snj}} & \frac{b_{13}^m}{\omega} + \sum_{snj} \frac{b_{snj13}}{\omega - c_{snj}} \\ \frac{b_{21}^m}{\omega} + \sum_{snj} \frac{b_{snj21}}{\omega - c_{snj}} & \frac{b_{22}^m}{\omega} + \sum_{snj} \frac{b_{snj22}}{\omega - c_{snj}} & \frac{b_{23}^m}{\omega} + \sum_{snj} \frac{b_{snj23}}{\omega - c_{snj}} \\ \frac{b_{31}^m}{\omega} + \sum_{snj} \frac{b_{snj31}}{\omega - c_{snj}} & \frac{b_{32}^m}{\omega} + \sum_{snj} \frac{b_{snj32}}{\omega - c_{snj}} & \frac{b_{33}^m}{\omega} + \sum_{snj} \frac{b_{snj33}}{\omega - c_{snj}} \end{pmatrix} \begin{pmatrix} \delta E_x \\ \delta E_y \\ \delta E_z \end{pmatrix}. \quad (8)$$

with coefficients

$$\begin{cases} b_{snj11} = \sum_{\sigma} r_{s\sigma} \omega_{ps}^2 p_{11snj} / c_{snj}, & b_{11}^m = -\sum_{s=m} \omega_{ps}^2 \sum_{\sigma} r_{s\sigma} [\sum_n A_{nbs\sigma} \frac{n\omega_{cs}}{k_x v_{\perp s\sigma}^2} (\frac{n\omega_{cs}}{k_x} + v_{dsx}) + \sum_{nj} p_{11snj} / c_{snj}], \\ b_{snj12} = \sum_{\sigma} r_{s\sigma} \omega_{ps}^2 p_{12snj} / c_{snj}, & b_{12}^m = -\sum_{s=m} \omega_{ps}^2 [\sum_{\sigma} r_{s\sigma} \sum_{nj} p_{12snj} / c_{snj}], \\ b_{snj21} = \sum_{\sigma} r_{s\sigma} \omega_{ps}^2 p_{21snj} / c_{snj}, & b_{21}^m = -\sum_{s=m} \omega_{ps}^2 [\sum_{\sigma} r_{s\sigma} \sum_{nj} p_{21snj} / c_{snj}], \\ b_{snj22} = \sum_{\sigma} r_{s\sigma} \omega_{ps}^2 p_{22snj} / c_{snj}, & b_{22}^m = -\sum_{s=m} \omega_{ps}^2 \sum_{\sigma} r_{s\sigma} [\sum_n (C_{nbs\sigma} + i \frac{v_{dsy}}{v_{\perp s\sigma}^2} B_{nbs\sigma}) + \sum_{nj} p_{22snj} / c_{snj}], \\ b_{snj13} = \sum_{\sigma} r_{s\sigma} \omega_{ps}^2 p_{13snj} / c_{snj}, & b_{13}^m = -\sum_{s=m} \omega_{ps}^2 [\sum_{\sigma} r_{s\sigma} \sum_{nj} p_{13snj} / c_{snj}], \\ b_{snj31} = \sum_{\sigma} r_{s\sigma} \omega_{ps}^2 p_{31snj} / c_{snj}, & b_{31}^m = -\sum_{s=m} \omega_{ps}^2 [\sum_{\sigma} r_{s\sigma} \sum_{nj} p_{31snj} / c_{snj}], \\ b_{snj23} = \sum_{\sigma} r_{s\sigma} \omega_{ps}^2 p_{23snj} / c_{snj}, & b_{23}^m = -\sum_{s=m} \omega_{ps}^2 [\sum_{\sigma} r_{s\sigma} \sum_{nj} p_{23snj} / c_{snj}], \\ b_{snj32} = \sum_{\sigma} r_{s\sigma} \omega_{ps}^2 p_{32snj} / c_{snj}, & b_{32}^m = -\sum_{s=m} \omega_{ps}^2 [\sum_{\sigma} r_{s\sigma} \sum_{nj} p_{32snj} / c_{snj}], \\ b_{snj33} = \sum_{\sigma} r_{s\sigma} \omega_{ps}^2 p_{33snj} / c_{snj}, & b_{33}^m = -\sum_{s=m} \omega_{ps}^2 \sum_{\sigma} r_{s\sigma} [\sum_n \frac{1}{2} A_{n0\sigma} + \sum_{nj} p_{33snj} / c_{snj}], \\ c_{snj} = c_{snj} = k_z v_{dsz} + n\omega_{cs} + k_x v_{dsx} - i v_s + k_z v_{zts} c_j. \end{cases} \quad (9)$$

The definition for variables in Eqs. (8) and (9) can be found in Ref. [1].

To implement Eq. (7), we need to separate the contribution from each species of $\delta \mathbf{J} = \sum_s \delta \mathbf{J}_s = \sum_s \boldsymbol{\sigma}_s \cdot \delta \mathbf{E}$. To do this, we use a relation of $\frac{b_{11}^m}{\omega} = \sum_s \frac{b_{11s}^m}{\omega}$, and then we rewrite Eqs. (8) and (9) as

$$\begin{aligned} \begin{pmatrix} \delta J_x^m \\ \delta J_y^m \\ \delta J_z^m \end{pmatrix} &= -i\epsilon_0 \begin{pmatrix} \sum_s \frac{b_{s11}^m}{\omega} + \sum_{snj} \frac{b_{snj11}}{\omega - c_{snj}} & \sum_s \frac{b_{s12}^m}{\omega} + \sum_{snj} \frac{b_{snj12}}{\omega - c_{snj}} & \sum_s \frac{b_{s13}^m}{\omega} + \sum_{snj} \frac{b_{snj13}}{\omega - c_{snj}} \\ \sum_s \frac{b_{s21}^m}{\omega} + \sum_{snj} \frac{b_{snj21}}{\omega - c_{snj}} & \sum_s \frac{b_{s22}^m}{\omega} + \sum_{snj} \frac{b_{snj22}}{\omega - c_{snj}} & \sum_s \frac{b_{s23}^m}{\omega} + \sum_{snj} \frac{b_{snj23}}{\omega - c_{snj}} \\ \sum_s \frac{b_{s31}^m}{\omega} + \sum_{snj} \frac{b_{snj31}}{\omega - c_{snj}} & \sum_s \frac{b_{s32}^m}{\omega} + \sum_{snj} \frac{b_{snj32}}{\omega - c_{snj}} & \sum_s \frac{b_{s33}^m}{\omega} + \sum_{snj} \frac{b_{snj33}}{\omega - c_{snj}} \end{pmatrix} \begin{pmatrix} \delta E_x \\ \delta E_y \\ \delta E_z \end{pmatrix} \\ &= \sum_s \boldsymbol{\sigma}_s^m \cdot \begin{pmatrix} \delta E_x \\ \delta E_y \\ \delta E_z \end{pmatrix} \end{aligned} \quad (10)$$

with the coefficients

$$\left\{ \begin{array}{l} b_{snj11} = \sum_{\sigma} r_{s\sigma} \omega_{ps}^2 p_{11snj} / c_{snj}, \quad b_{s11}^m = -\omega_{ps}^2 \sum_{\sigma} r_{s\sigma} [\sum_n A_{nbs\sigma} \frac{n\omega_{cs}}{k_x v_{Ls\sigma}^2} (\frac{n\omega_{cs}}{k_x} + v_{dsx}) + \sum_{nj} p_{11snj} / c_{snj}], \\ b_{snj12} = \sum_{\sigma} r_{s\sigma} \omega_{ps}^2 p_{12snj} / c_{snj}, \quad b_{s12}^m = -\omega_{ps}^2 [\sum_{\sigma} r_{s\sigma} \sum_{nj} p_{12snj} / c_{snj}], \\ b_{snj21} = \sum_{\sigma} r_{s\sigma} \omega_{ps}^2 p_{21snj} / c_{snj}, \quad b_{s21}^m = -\omega_{ps}^2 [\sum_{\sigma} r_{s\sigma} \sum_{nj} p_{21snj} / c_{snj}], \\ b_{snj22} = \sum_{\sigma} r_{s\sigma} \omega_{ps}^2 p_{22snj} / c_{snj}, \quad b_{s22}^m = -\omega_{ps}^2 \sum_{\sigma} r_{s\sigma} [\sum_n (C_{nbs\sigma} + i \frac{v_{dsy}}{v_{Ls\sigma}} B_{nbs\sigma}) + \sum_{nj} p_{22snj} / c_{snj}], \\ b_{snj13} = \sum_{\sigma} r_{s\sigma} \omega_{ps}^2 p_{13snj} / c_{snj}, \quad b_{s13}^m = -\omega_{ps}^2 [\sum_{\sigma} r_{s\sigma} \sum_{nj} p_{13snj} / c_{snj}], \\ b_{snj31} = \sum_{\sigma} r_{s\sigma} \omega_{ps}^2 p_{31snj} / c_{snj}, \quad b_{s31}^m = -\omega_{ps}^2 [\sum_{\sigma} r_{s\sigma} \sum_{nj} p_{31snj} / c_{snj}], \\ b_{snj23} = \sum_{\sigma} r_{s\sigma} \omega_{ps}^2 p_{23snj} / c_{snj}, \quad b_{s23}^m = -\omega_{ps}^2 [\sum_{\sigma} r_{s\sigma} \sum_{nj} p_{23snj} / c_{snj}], \\ b_{snj32} = \sum_{\sigma} r_{s\sigma} \omega_{ps}^2 p_{32snj} / c_{snj}, \quad b_{s32}^m = -\omega_{ps}^2 [\sum_{\sigma} r_{s\sigma} \sum_{nj} p_{32snj} / c_{snj}], \\ b_{snj33} = \sum_{\sigma} r_{s\sigma} \omega_{ps}^2 p_{33snj} / c_{snj}, \quad b_{s33}^m = -\omega_{ps}^2 \sum_{\sigma} r_{s\sigma} [\sum_n \frac{1}{2} A_{n0\sigma} + \sum_{nj} p_{33snj} / c_{snj}], \\ c_{snj} = c_{snj} = k_z v_{dsz} + n\omega_{cs} + k_x v_{dsx} - iv_s + k_z v_{zts} c_j. \end{array} \right. \quad (11)$$

Consequently, we have

$$\delta \mathbf{J}_s^m = \boldsymbol{\sigma}_s^m \cdot \delta \mathbf{E}, \quad \boldsymbol{\sigma}_s^m = -i\epsilon_0 \begin{pmatrix} \frac{b_{s11}^m}{\omega} + \sum_{nj} \frac{b_{snj11}}{\omega - c_{snj}} & \frac{b_{s12}^m}{\omega} + \sum_{nj} \frac{b_{snj12}}{\omega - c_{snj}} & \frac{b_{s13}^m}{\omega} + \sum_{nj} \frac{b_{snj13}}{\omega - c_{snj}} \\ \frac{b_{s21}^m}{\omega} + \sum_{nj} \frac{b_{snj21}}{\omega - c_{snj}} & \frac{b_{s22}^m}{\omega} + \sum_{nj} \frac{b_{snj22}}{\omega - c_{snj}} & \frac{b_{s23}^m}{\omega} + \sum_{nj} \frac{b_{snj23}}{\omega - c_{snj}} \\ \frac{b_{s31}^m}{\omega} + \sum_{nj} \frac{b_{snj31}}{\omega - c_{snj}} & \frac{b_{s32}^m}{\omega} + \sum_{nj} \frac{b_{snj32}}{\omega - c_{snj}} & \frac{b_{s33}^m}{\omega} + \sum_{nj} \frac{b_{snj33}}{\omega - c_{snj}} \end{pmatrix}. \quad (12)$$

We can use Eq. (12) to obtain $\delta \mathbf{J}_s$. Since $\delta \mathbf{E}$ is known, the first approach requires solving the above 3-by-3 tensor for each species.

The second approach would be more convenient for obtaining $\delta \mathbf{J}_s$ based on the fact that a matrix eigenvalue method is used in BO/PDRK. For example, as given in Eq. (132) of Ref. [1], the perturbed current in x direction is

$$i\delta J_x \epsilon_0 = j_x + \sum_{snj}^{s=m} v_{snjx} + \sum_{sj\sigma}^{s=u} v_{sj\sigma x}, \quad (13)$$

where j_x , v_{snjx} and $v_{sj\sigma x}$ have been solved along with $\delta \mathbf{E}$ and $\delta \mathbf{B}$. δJ_{sx} can be directly obtained once j_x , v_{snjx} and $v_{sj\sigma x}$ for each species s are known. Similarly, we can obtain δJ_{sy} and δJ_{sz} .

The quantities v_{snjx} and $v_{sj\sigma x}$ are species quantities, but j_x was not in the original version of BO/PDRK. With the addition of only $S - 1$ matrix elements, we can replace the matrix element j_x by a sum over S matrix elements j_{sx} , where S is the number of species. To do this, we modified the BO/PDRK matrix equations in Eq. (10), i.e.,

$$\begin{cases} \omega j_x = b_{11} \delta E_x + b_{12} \delta E_y + b_{13} \delta E_z, \\ \omega j_y = b_{21} \delta E_x + b_{22} \delta E_y + b_{23} \delta E_z, \\ \omega j_z = b_{31} \delta E_x + b_{32} \delta E_y + b_{33} \delta E_z, \end{cases} \quad (14)$$

as

$$\begin{cases} \omega j_{sx} = b_{s11} \delta E_x + b_{s12} \delta E_y + b_{s13} \delta E_z, \\ \omega j_{sy} = b_{s21} \delta E_x + b_{s22} \delta E_y + b_{s23} \delta E_z, \\ \omega j_{sz} = b_{s31} \delta E_x + b_{s32} \delta E_y + b_{s33} \delta E_z. \end{cases} \quad (15)$$

This separation can directly give $j_{sx,y,z}$ from the BO/PDRK matrix, which then yields $\delta J_{sx,y,z}$ through the following equations

$$\begin{cases} \delta J_{sx} = (j_{sx} + \sum_{nj}^{s=m} v_{snjx} + \sum_{j\sigma}^{s=u} v_{sj\sigma x}) / (i\epsilon_0), \\ \delta J_{sy} = (j_{sy} + \sum_{nj}^{s=m} v_{snjy} + \sum_{j\sigma}^{s=u} v_{sj\sigma y}) / (i\epsilon_0), \\ \delta J_{sz} = (j_{sz} + \sum_{nj}^{s=m} v_{snjz} + \sum_{j\sigma}^{s=u} v_{sj\sigma z}) / (i\epsilon_0). \end{cases} \quad (16)$$

The updated matrix equations of BO, i.e., Eq.(132) of Ref.[1], become

$$\left\{ \begin{array}{l}
\omega v_{snjx}^{s=m} = c_{snj} v_{snjx} + b_{snj11} \delta E_x + b_{snj12} \delta E_y + b_{snj13} \delta E_z, \\
\omega v_{sj\sigma x}^{s=u} = c_{sj\sigma} v_{sj\sigma x} + b_{sj\sigma 11} \delta E_x + b_{sj\sigma 12} \delta E_y + b_{sj\sigma 13} \delta E_z, \\
\omega j_{sx} = b_{s11} \delta E_x + b_{s12} \delta E_y + b_{s13} \delta E_z, \\
i\delta J_x / \epsilon_0 = j_x + \sum_{snj}^{s=m} v_{snjx} + \sum_{sj\sigma}^{s=u} v_{sj\sigma x}, \\
\omega v_{snjy}^{s=m} = c_{snj} v_{snjy} + b_{snj21} \delta E_x + b_{snj22} \delta E_y + b_{snj23} \delta E_z, \\
\omega v_{sj\sigma y}^{s=u} = c_{sj\sigma} v_{sj\sigma y} + b_{sj\sigma 21} \delta E_x + b_{sj\sigma 22} \delta E_y + b_{sj\sigma 23} \delta E_z, \\
\omega j_{sy} = b_{s21} \delta E_x + b_{s22} \delta E_y + b_{s23} \delta E_z, \\
i\delta J_y / \epsilon_0 = j_y + \sum_{snj}^{s=m} v_{snjy} + \sum_{sj\sigma}^{s=u} v_{sj\sigma y}, \\
\omega v_{snjz}^{s=m} = c_{snj} v_{snjz} + b_{snj31} \delta E_x + b_{snj32} \delta E_y + b_{snj33} \delta E_z, \\
\omega v_{sj\sigma z}^{s=u} = c_{sj\sigma} v_{sj\sigma z} + b_{sj\sigma 31} \delta E_x + b_{sj\sigma 32} \delta E_y + b_{sj\sigma 33} \delta E_z, \\
\omega j_{sz} = b_{s31} \delta E_x + b_{s32} \delta E_y + b_{s33} \delta E_z, \\
i\delta J_z / \epsilon_0 = j_z + \sum_{snj}^{s=m} v_{snjz} + \sum_{sj\sigma}^{s=u} v_{sj\sigma z}, \\
\omega \delta E_x = c^2 k_z \delta B_y - i\delta J_x / \epsilon_0, \\
\omega \delta E_y = -c^2 k_z \delta B_x + c^2 k_x \delta B_z - i\delta J_y / \epsilon_0, \\
\omega \delta E_z = -c^2 k_x \delta B_y - i\delta J_z / \epsilon_0, \\
\omega \delta B_x = -k_z \delta E_y, \\
\omega \delta B_y = k_z \delta E_x - k_x \delta E_z, \\
\omega \delta B_z = k_x \delta E_y,
\end{array} \right. \quad (17)$$

which yields a sparse matrix eigenvalue problem $\omega \mathbf{X} = \mathbf{M}(\mathbf{k}) \cdot \mathbf{X}$. The symbols such as v_{snjx} , $j_{sx,y,z}$ and $\delta J_{x,y,z}$ used here are analogous to the perturbed velocity and current density in fluid derivations of plasma waves. The elements of the eigenvector $(\delta E_x, \delta E_y, \delta E_z, \delta B_x, \delta B_y, \delta B_z)$ represent the perturbed electric and magnetic fields. Thus, all variables of one plasma wave mode can be obtained in a straightforward manner. In addition, the dimension of the matrix is $N_N = 3 \times (N_{SmN} + N_{SuJ} + S) + 6 = 3 \times \{[S_m \times (2 \times N + 1) + S_u \times 2] \times J + S\} + 6$, where S_m and S_u are the numbers of magnetized and unmagnetized species, respectively, $S = S_m + S_u$, N is the number of harmonics retained for magnetized species, and J is the order of the J -pole expansion used for calculation of the plasma dispersion Z function.

2.3. Benchmark strategies

In order to test whether the values of $(\delta \mathbf{E}, \delta \mathbf{B}, \delta \mathbf{J}, \delta \mathbf{J}_s, \delta n_s, \delta \mathbf{v}_s)$ calculated by BO are correct, we do the following benchmarks:

- (1) Use $\omega \delta \mathbf{B} = \mathbf{k} \times \delta \mathbf{E}$ to check $\delta \mathbf{B}$ and $\delta \mathbf{J} = \frac{1}{\mu_0} i \mathbf{k} \times \delta \mathbf{B} + i \epsilon_0 \omega \delta \mathbf{E}$ to check $\delta \mathbf{J}$.
- (2) Use $\delta \mathbf{J}_s = \boldsymbol{\sigma}_s \cdot \delta \mathbf{E}$ to calculate $\delta \mathbf{J}_s$ and $\delta \mathbf{J} = \sum_s \delta \mathbf{J}_s$ to calculate $\delta \mathbf{J}$, and compare this with $\delta \mathbf{J}$ from (1).
- (3) Compare $\delta \mathbf{J}_s$ and $\delta \mathbf{J}$ in (2) with the analogous quantities calculated in the new version of BO/PDRK using $j_{sx,y,z}$ and v_{snj} .
- (4) Write out 3-by-3 tensors $\boldsymbol{\sigma}_s$, \mathbf{Q}_s , $\boldsymbol{\sigma}$, \mathbf{Q} , \mathbf{K} and $\mathbf{D}(\omega, \mathbf{k})$ and verify that $|\mathbf{D}(\omega, \mathbf{k})| = 0$.
- (5) Compare values of $\delta \mathbf{J}_s$, $\delta \mathbf{J}$, δn_s and $\delta \mathbf{v}_s$ with those calculated using jWHAMP and the multi-fluid solver PDRF.

Using the new version of BO, we have checked the above (1)-(4) in several test cases and have identified a good consistence between these two methods proposed in Subsection 2.2. In following Section, we will present benchmark results in the above (5).

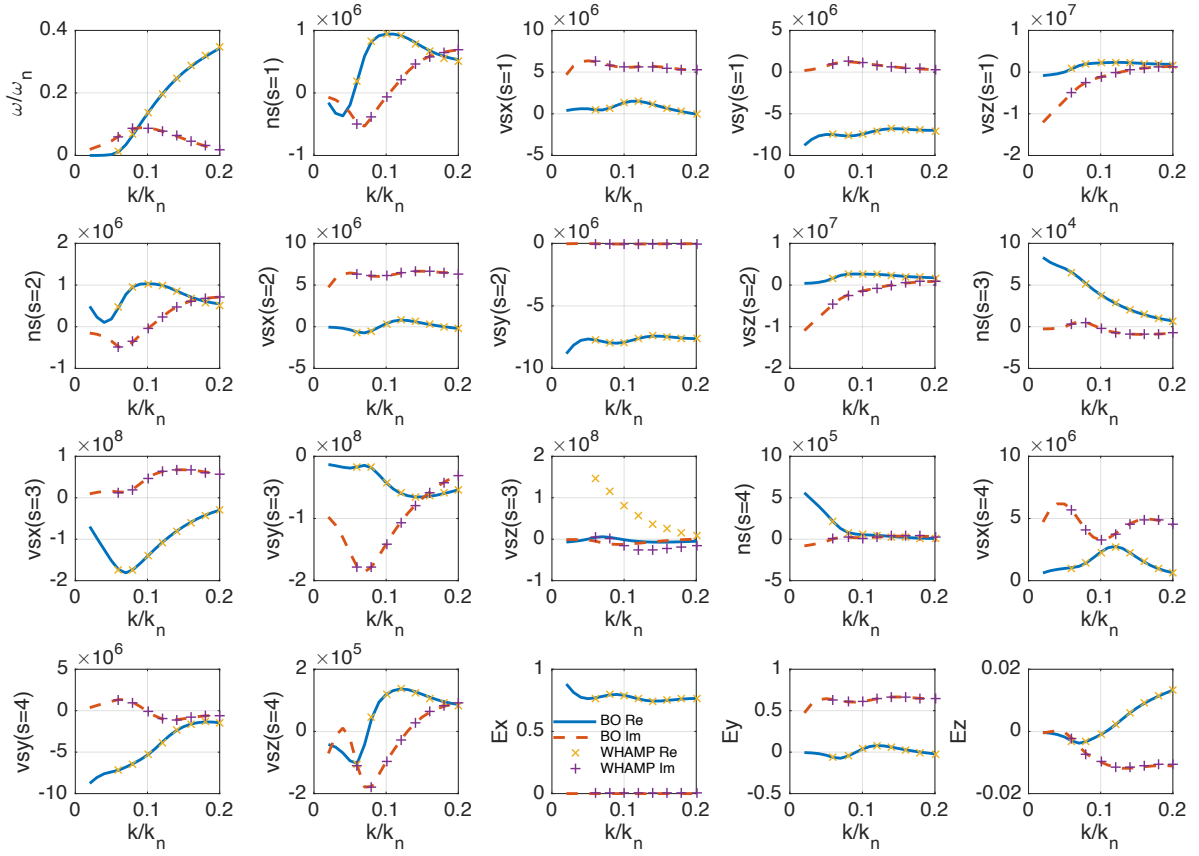


Figure 1: Comparison of results from BO and jWHAMP with parameters case#1. All of the quantities calculated by these two codes agree well except for $\delta v_z(s=3)$. BO contains the effect relating to v_{dsz} for species 3, whereas $v_{dsz} \neq 0$ was not taken into account in the current version of jWHAMP.

3. Benchmark and comparing with multi-fluid plasma model

3.1. Benchmark with jWHAMP

jWHAMP is Dartmouth College's java extension of the WHAMP electromagnetic dispersion code [6], which export a number of polarization quantities such as $(\delta E, \delta B, \delta n_s, \delta v_s)$. However, in jWHAMP, the drift velocity, v_{ds} , was not taken into account when calculating δv_s . To test the greatest number of features of a kinetic calculation, we consider a case (case#1) where the plasma consists of four species. We also consider both parallel and perpendicular components of the wave vector in case#1. The input species parameters for this case (specified in the 'bo.in' input file) are

qs (e)	ms(m_unit)	ns(m ⁻³)	Tzs(eV)	Tps(eV)	vdsz/c
1	1	1e6	24.838e3	99.352e3	0.0
-1	5.447e-4	1.11e6	24.838e3	24.838e3	0.0
1	1	0.01e6	24.838e4	24.838e4	0.0727
1	4	0.1e6	0.1e3	0.1e3	0.0

Here, we use the default normalization in BO: the mass m_s is normalized to the proton mass m_p , k_x and k_z are normalized to $k_n = \omega_{ps1}/c$ and the frequency is normalized to $\omega_n = |\omega_{cs1}|$, where "1" indicates the first species (i.e., the proton component with $n_s = 10^6 \text{ m}^{-3}$). The case#1 contains both anisotropic temperature and parallel drift velocity effects, which would destabilize the Alfvén/ion-cyclotron mode wave as shown in Fig. 1 that presents the distributions of the real and imaginary parts of frequency ω , δn_s , δv_s and δE as a function of k_z under $k_x = 0.05$ and $B_0 = 100 \text{ nT}$.

For all quantities presented in Fig. 1, both BO and jWHAMP give the same distributions except for the values of $\delta v_z(s=3)$. The reason is that the effect of the drift was not included in jWHAMP to calculate δv_z . If we ignore v_{dsz} in Eq. (7), we find that $\delta v_z(s=3)$ from BO agrees with the value from jWHAMP.

This benchmark indicates that the new version of BO can correctly give the perturbed density and velocity in case#1. Moreover, the comparison between BO and jWHAMP shows that it needs to take into account v_{ds} for calculating the perturbed velocity.

3.2. Comparing with multi-fluid plasma model

Here we compare the results of BO with those of a multi-fluid model. In the cold plasma limit ($v_{zts}, v_{\perp ts} \approx 0$ or $\omega \gg k_z v_{zts}$), the kinetic results and fluid results should be identical. Note that we have updated the multi-fluid plasma dispersion relation solver PDRF, and that it can be run in the new version of BO (see Appendix A).

Fig. 2 compares results from the BO kinetic and fluid models for a cold four species plasma where $B_0 = 2000 \text{ nT}$. The results are shown as a function of k for the most unstable mode wave which has the wave normal angle $\theta = 10^\circ$. The input parameters for this case (case#2) are

qs (e)	ms(m_unit)	ns(m ⁻³)	Tzs(eV)	Tps(eV)	vdsz/c	vdsx/c	vdsy/c
1	1	0.8e10	1.0e-1	1.0e-1	0.0	0.0	0.0
1	1	0.1e10	1.0e-1	1.0e-1	2.0e-3	3.0e-3	1.0e-3
2	4	0.05e10	1.0e-1	1.0e-1	0.0	0.0	0.0
-1	5.447e-4	1.0e10	1.0e-1	1.0e-1	2.0e-4	3.0e-4	1.0e-4

We consider both parallel and perpendicular beams in case#2, and the default normalization is used. Fig. 2 shows that both kinetic and fluid models give the nearly same results. For large k ($\sim 5k_n$), there is a slight difference between ω_i for the the kinetic and fluid models, due to Landau damping in the kinetic model. If we decrease the temperature to 0.01 eV, the deviation nearly vanishes. These results indicate that the equations in Sec.2 and there implementation in BO are correct, even including perpendicular beams.

We further compare results from the fluid and kinetic models for a warm plasma with isotropic pressure. The species parameters for this case (case#3) are

qs (e)	ms(m_unit)	ns(m ⁻³)	Tzs(eV)	Tps(eV)
1	1	0.36e8	24.838e1	24.838e1
-1	5.447e-4	0.36e8	1.0	1.0

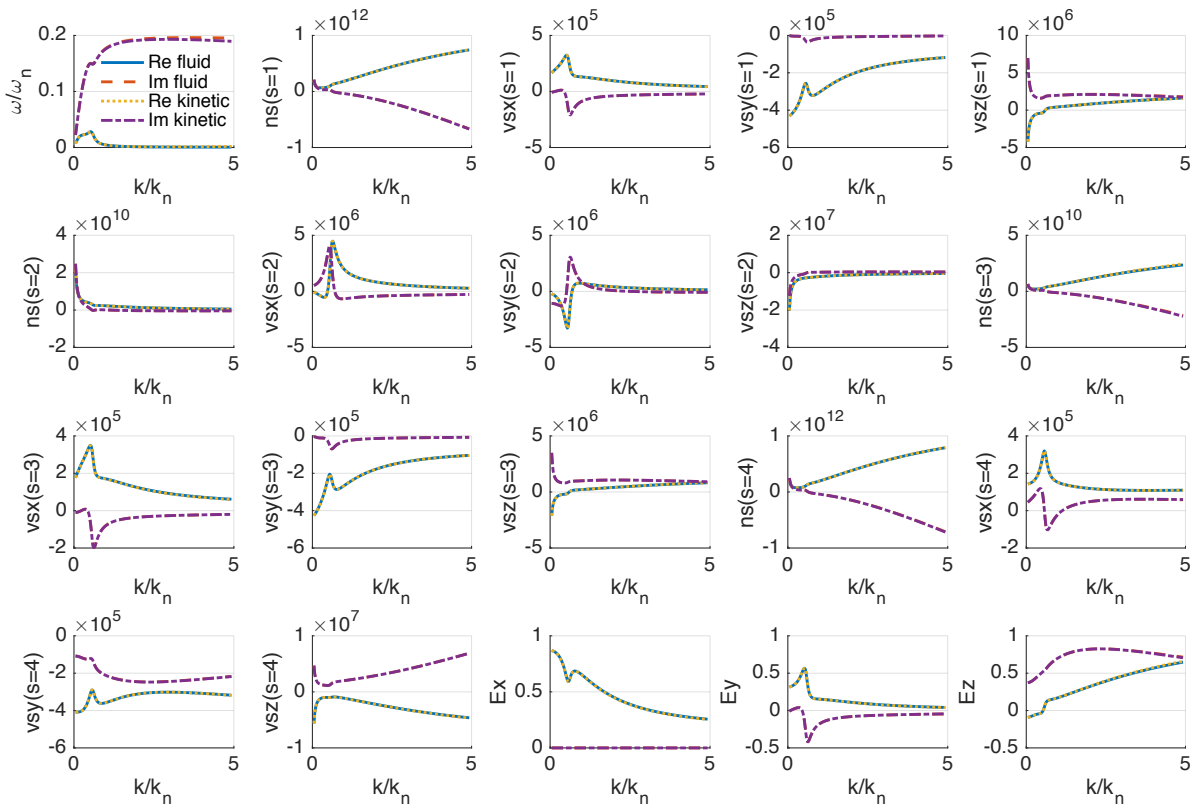


Figure 2: Comparison of results from the BO kinetic and multi-fluid models for a cold plasma with parameters case#2. The wave is the most unstable mode with the wave normal angle $\theta = 10^\circ$. All quantities calculated using these two models agree well.

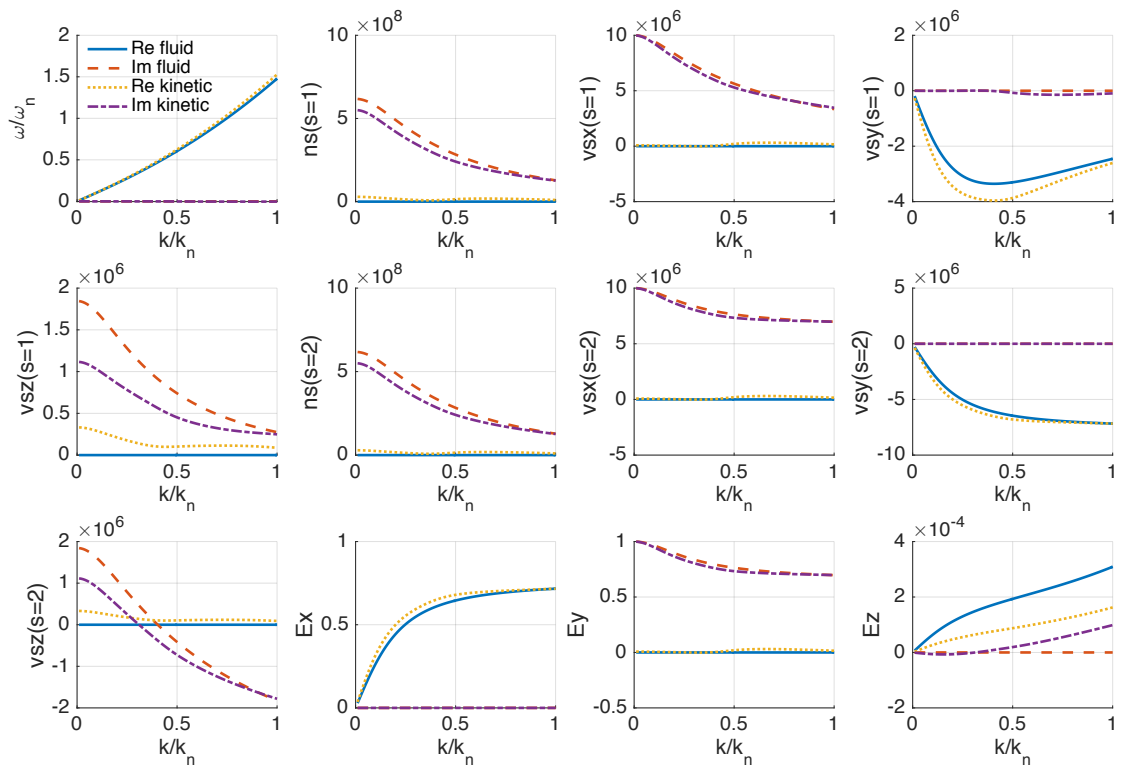


Figure 3: Comparison of BO kinetic and fluid results for the fast-magnetosonic/whistler mode wave with parameters case#3.

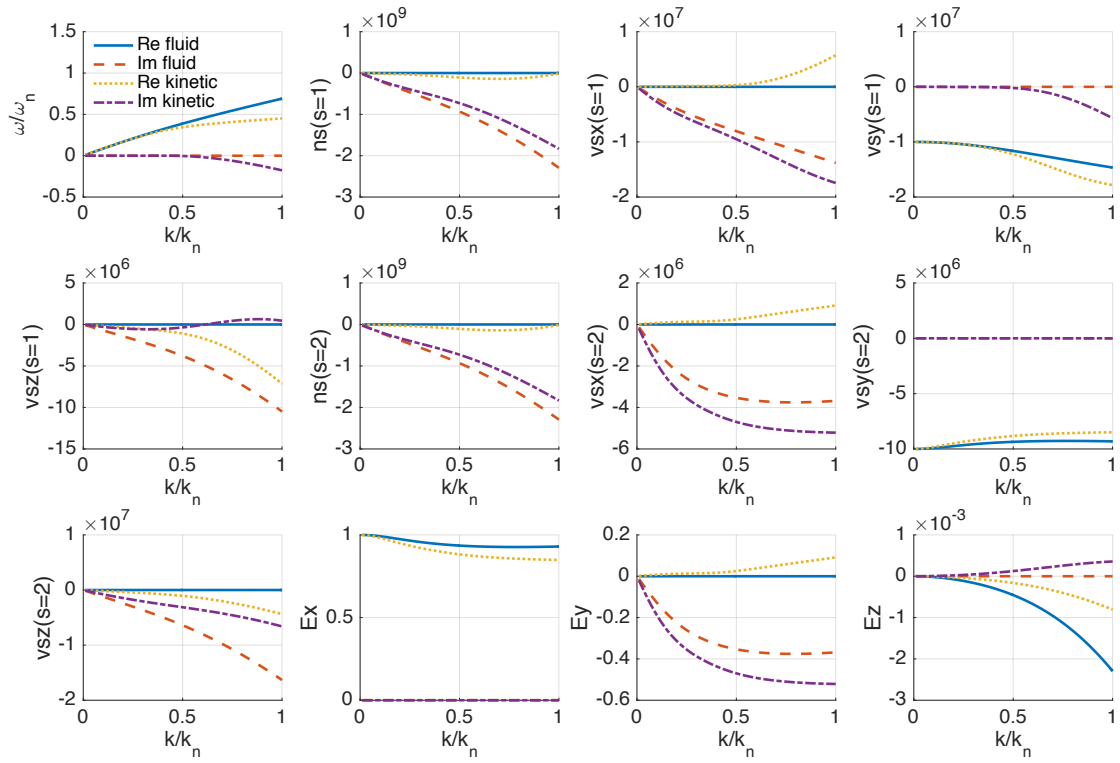


Figure 4: Comparison of BO kinetic and fluid results for the Alfvén/ion-cyclotron mode wave with parameters case#3. This wave is strongly damped at large k in the kinetic model due to wave-particle interactions.

In order to have the consistent sound speed in both kinetic and fluid models, i.e., $c_s^2 \approx v_{ts}^2$, we choose the default adiabatic pressure closure with adiabatic coefficients $\gamma_{\parallel s} = \gamma_{\perp s} = 2.0$. We also use $B_0 = 100$ nT and $\theta = 30^\circ$. Figs. 3 and 4 give the results of the fast-magnetosonic/whistler mode and the Alfvén/ion-cyclotron mode, respectively. Since the kinetic wave-particle interactions considerably enhance in the warm plasma, the kinetic results would be different from the fluid results. Fig.3 shows that although the wave frequency from the kinetic and fluid models is almost the same, the quantities $(\delta\mathbf{E}, \delta\mathbf{B}, \delta n_s, \delta\mathbf{v}_s)$ have much larger deviations. Fig.4 shows that both the wave frequency and polarization have significant differences.

4. Summary and discussions

In this paper, we describe the updated BO plasma wave dispersion relation solver that can be used for both kinetic and fluid plasma models. We extend the kinetic version to obtain density and velocity perturbations for each species. In the cold plasma limit, the kinetic model yields results of $(\mathbf{k}, \omega, \delta\mathbf{E}, \delta\mathbf{B}, \delta\mathbf{J}, \delta n_s, \delta\mathbf{v}_s)$ quite similar to those from the multi-fluid model, even for zeroth order drift beams in arbitrary directions. In a warm plasma, Landau and cyclotron wave-particle resonance effects can alter the wave frequency and the polarization, which induce the difference between the kinetic and fluid models. The extensive set of polarization quantities calculated by the updated BO (see Appendix B) could be useful for identifying and characterizing plasma waves and instabilities in space plasmas.

Acknowledgments Work at Dartmouth College was supported by NASA grant 80NSSC19K0270.

Appendix A. Reduced version of multi-fluid plasma dispersion relation solver PDRF

To make the PDRF code more amenable to comparison with BO-K/PDRK, we simplify the original version of PDRF by removing density inhomogeneity, relativistic effects and collisions, and make it available as BO-F in BO code. Drifts in arbitrary directions and pressure anisotropy are retained. Some typos in Ref.[3] are also corrected here.

We consider a multi-fluid plasma in an external magnetic field $\mathbf{B}_0 = (0, 0, B_0)$. The zero-th order flow velocity of the fluid component s is $\mathbf{v}_{ds} = (v_{dsx}, v_{dsy}, v_{dsz})$. The species densities and temperatures are homogeneous, i.e., gradient effects are ignored, and the wave vector is assumed to be $\mathbf{k} = (k_x, 0, k_z) = (k \sin \theta, 0, k \cos \theta)$.

We start with the multi-fluid equations

$$\partial_t n_s = -\nabla \cdot (n_s \mathbf{v}_s), \quad (\text{A.1a})$$

$$\partial_t \mathbf{v}_s = -\mathbf{v}_s \cdot \nabla \mathbf{v}_s + \frac{q_s}{m_s} (\mathbf{E} + \mathbf{v}_s \times \mathbf{B}) - \frac{\nabla P_s}{\rho_s}, \quad (\text{A.1b})$$

$$\partial_t \mathbf{E} = c^2 \nabla \times \mathbf{B} - \mathbf{J} / \epsilon_0, \quad (\text{A.1c})$$

$$\partial_t \mathbf{B} = -\nabla \times \mathbf{E}, \quad (\text{A.1d})$$

where we ignore the relativistic effects, and

$$\mathbf{J} = \sum_s q_s n_s \mathbf{v}_s, \quad (\text{A.2a})$$

$$d_t (P_{\parallel, \perp s} \cdot \rho_s^{-\gamma_{\parallel, \perp s}}) = 0, \quad (\text{A.2b})$$

where the mass density is $\rho_s \equiv m_s n_s$, and the speed of light is $c = 1 / \sqrt{\mu_0 \epsilon_0}$. In the above equations, we have used adiabatic model for pressure closure, with $\gamma_{\parallel, \perp s}$ being the parallel and perpendicular exponents. Furthermore, $P_{\parallel, \perp} = nk_B T_{\parallel, \perp}$, $\mathbf{P} = P_{\parallel} \hat{\mathbf{b}} \hat{\mathbf{b}} + P_{\perp} (\mathbf{I} - \hat{\mathbf{b}} \hat{\mathbf{b}})$ and $\hat{\mathbf{b}} = \mathbf{B} / B$. Different anisotropic pressure closures will yield different results. Usually, one take $\gamma_{\parallel} = \gamma_{\perp} = 5/3$. However, we find $\gamma_{\parallel} = \gamma_{\perp} = 2$ would yield closer results to those of the kinetic model. If not specified by the user, $\gamma_{\parallel} = \gamma_{\perp} = 2$ are the default settings.

After linearizing, (A.2) becomes

$$\delta \mathbf{J} = \sum_s q_s (n_{s0} \delta \mathbf{v}_s + \delta n_s \mathbf{v}_{ds}), \quad (\text{A.3a})$$

$$\delta P_{\parallel, \perp s} = P_{\parallel, \perp s0} \gamma_{\parallel, \perp s} \delta n_s / n_{s0} = c_{\parallel, \perp s}^2 m_s \delta n_s, \quad (\text{A.3b})$$

where $c_{\parallel,\perp s}^2 \equiv \gamma_{\parallel,\perp s} P_{\parallel,\perp s 0} / \rho_{s0}$ and $P_{s0} = n_{s0} k_B T_{s0}$. We also define $c_{As} \equiv B_0^2 / (\mu_0 \rho_{s0})$. We have

$$\nabla \cdot \delta \mathbf{P}_s = (ik_x, 0, ik_z) \cdot \begin{bmatrix} \delta P_{\perp s} & 0 & \Delta_s \delta B_x \\ 0 & \delta P_{\perp s} & \Delta_s \delta B_y \\ \Delta_s \delta B_x & \Delta_s \delta B_y & \delta P_{\parallel s} \end{bmatrix} = \begin{pmatrix} ik_x \delta P_{\perp s} + ik_z \Delta_s \delta B_x \\ ik_z \Delta_s \delta B_y \\ ik_x \Delta_s \delta B_x + ik_z \delta P_{\parallel s} \end{pmatrix}^T, \quad (\text{A.4})$$

where $\Delta_s \equiv (P_{\parallel s 0} - P_{\perp s 0}) / B_0$ and $\beta_{\parallel,\perp s} = 2\mu_0 P_{\parallel,\perp s} / B_0^2$. The off-diagonal terms coming from the tensor rotation from $\hat{\mathbf{b}}_0$ to $\hat{\mathbf{b}}$ are related to energy exchange and are important for the anisotropic instabilities.

The linearized version of (A.1) with $f = f_0 + \delta f e^{ik \cdot r - i\omega t}$, $\delta f \ll f_0$ is equivalent to a matrix eigenvalue problem

$$\omega \mathbf{X} = \mathbf{M} \mathbf{X}, \quad (\text{A.5})$$

where ω is the eigenvalue and \mathbf{X} is the corresponding eigenvector containing polarization information for the eigenvectors. Accordingly, we have $\mathbf{X} = (\delta n_s, \delta v_{sx}, \delta v_{sy}, \delta v_{sz}, \delta E_x, \delta E_y, \delta E_z, \delta B_x, \delta B_y, \delta B_z)^T$, and the matrix

$$\mathbf{M} = \begin{pmatrix} \left\{ \begin{array}{cccc} \mathbf{k} \cdot \mathbf{v}_{ds} & k_x n_{s0} & 0 & k_z n_{s0} \\ \frac{k_x c_{\perp s}^2}{n_{s0}} & \mathbf{k} \cdot \mathbf{v}_{ds} & i\omega_{cs} & 0 \\ 0 & -i\omega_{cs} & \mathbf{k} \cdot \mathbf{v}_{ds} & 0 \\ \frac{k_z c_{\perp s}^2}{n_{s0}} & 0 & 0 & \mathbf{k} \cdot \mathbf{v}_{ds} \end{array} \right\} & \left\{ \begin{array}{cccc} 0 & 0 & 0 & 0 \\ i\frac{q_s}{m_s} & 0 & 0 & \frac{k_z \Delta_s}{m_s n_{s0}} \\ 0 & i\frac{q_s}{m_s} & 0 & i\frac{q_s v_{dsz}}{m_s} \\ 0 & 0 & i\frac{q_s}{m_s} & -i\frac{q_s v_{dsy}}{m_s} + \frac{k_x \Delta_s}{m_s n_{s0}} \end{array} \right\} & \left\{ \begin{array}{cccc} 0 & 0 & 0 & 0 \\ 0 & 0 & 0 & 0 \\ 0 & 0 & 0 & 0 \\ 0 & 0 & 0 & 0 \\ 0 & 0 & 0 & 0 \\ 0 & 0 & 0 & 0 \\ 0 & 0 & 0 & 0 \\ 0 & 0 & 0 & 0 \\ 0 & 0 & 0 & 0 \end{array} \right\} & \left\{ \begin{array}{cccc} 0 & 0 & 0 & 0 \\ 0 & 0 & 0 & 0 \\ 0 & 0 & 0 & 0 \\ 0 & 0 & 0 & 0 \\ 0 & 0 & 0 & 0 \\ 0 & 0 & 0 & 0 \\ 0 & 0 & 0 & 0 \\ 0 & 0 & 0 & 0 \\ 0 & 0 & 0 & 0 \end{array} \right\} \end{pmatrix}, \quad (\text{A.6})$$

where that the elements between ‘{’ and ‘}’ means each species s has its own matrix elements, $\omega_{cs} = q_s B_0 / m_s$, $q_e = -e$, $\omega_{ps}^2 = n_{s0} q_s^2 / (\epsilon_0 m_s)$, and $\mathbf{k} \cdot \mathbf{v}_{ds} = k_x v_{dsx} + k_z v_{dsz}$. For a plasma containing S species, the dimension of \mathbf{M} is $(4S + 6) \times (4S + 6)$. If we define the thermal velocity $v_{\parallel,\perp s} = \sqrt{2k_B T_{\parallel,\perp s} / m_s}$ as in the kinetic version of BO[1], we can have $c_{\parallel,\perp s} = \sqrt{\gamma_{\parallel,\perp s} / 2} v_{\parallel,\perp s}$, or the temperature $k_B T_{\parallel,\perp s 0} = m_s c_{\parallel,\perp s}^2 / \gamma_{\parallel,\perp s}$.

We can also use some other pressure closures. For example, the double-polytropic laws for pressure closure

$$d_t(P_{\parallel s} \cdot \rho_s^{-\gamma_{\parallel s}} \cdot B^{\gamma_{\parallel s}-1}) = 0, \quad (\text{A.7a})$$

$$d_t(P_{\perp s} \cdot \rho_s^{-1} \cdot B^{-\gamma_{\perp s}+1}) = 0, \quad (\text{A.7b})$$

with γ_{\parallel} and $\gamma_{\perp s}$ being the parallel and perpendicular polytropic exponents had been used previously in space plasma studies, c.f., Ref.[9]. Note that $\gamma_{\parallel} = 3$ and $\gamma_{\perp} = 2$ yield the CGL relations[10], whereas $\gamma_{\parallel} = \gamma_{\perp} = 1$ yields isothermal behavior. For this pressure closure, we have

$$\delta P_{\parallel s} = P_{\parallel s 0} [\gamma_{\parallel s} \delta n_s / n_{s0} - (\gamma_{\parallel s} - 1) \delta B_z / B_0] = c_{\parallel s}^2 m_s \delta n_s - P_{\parallel s 0} (\gamma_{\parallel s} - 1) \delta B_z / B_0, \quad (\text{A.8a})$$

$$\delta P_{\perp s} = P_{\perp s 0} [\delta n_s / n_{s0} + (\gamma_{\perp s} - 1) \delta B_z / B_0] = c_{\perp s}^2 m_s \delta n_s + P_{\perp s 0} (\gamma_{\perp s} - 1) \delta B_z / B_0, \quad (\text{A.8b})$$

where $c_{\parallel s}^2 \equiv \gamma_{\parallel s} P_{\parallel s 0} / \rho_{s0}$ and $c_{\perp s}^2 \equiv P_{\perp s 0} / \rho_{s0}$ (here is different from the $c_{\perp s}^2 \equiv \gamma_{\perp} P_{\perp s 0} / \rho_{s0}$ in Ref.[9]), and hence the matrix elements $M_{\delta v_{sx}, \delta n_s}$, $M_{\delta v_{sx}, \delta B_z}$ and $M_{\delta v_{sz}, \delta B_z}$ in \mathbf{M} would be modified accordingly. Similarly to the adiabatic pressure closure case, we can have $c_{\parallel s} = \sqrt{\gamma_{\parallel s} / 2} v_{\parallel s}$ and $c_{\perp s} = \sqrt{1/2} v_{\perp s}$, or the temperature $k_B T_{\parallel s 0} = m_s c_{\parallel s}^2 / \gamma_{\parallel s}$ and $k_B T_{\perp s 0} = m_s c_{\perp s}^2$.

In BO, because of the limitations of the pressure closure, we only use the above fluid version to get a rough description of the waves and instabilities and for comparison with the kinetic version. It is especially useful for studying cold plasma waves and beam modes, in which case the pressure closure is not important. The fluid closure has many limitations and leads to some un-physical results. For example, in the double-polytropic CGL case ($\gamma_{\parallel} = 3$, $\gamma_{\perp} = 2$), the waves can be unstable even when $P_{\parallel} = P_{\perp s 0} = P_{\parallel s 0}$ because $c_{\parallel s}^2 \neq c_{\perp s}^2$. The high beta anisotropic firehose and mirror mode instabilities are also difficult to calculate accurately from fluid model. For accurate results with finite pressure, we recommend the kinetic version of BO.

Appendix B. Polarizations in BO

For given real k_x, k_z and corresponding complex ω , we find the complex quantities $\delta E_x, \delta E_y, \delta E_z, \delta B_x, \delta B_y, \delta B_z, \delta J_x, \delta J_y, \delta J_z, \delta J_{sx}, \delta J_{sy}, \delta J_{sz}, \delta n_s, \delta v_{sx}, \delta v_{sy}, \delta v_{sz}$. We list the comprehensive polarization quantities calculated in the new version of BO code, and summarize them in Table B.1. Note that for a given (k_x, k_z) , there exist multiple branches corresponding to different eigenmodes ω , and each branch has its unique polarization.

Table B.1: List of the polarization quantities in BO. The numbers before each polarizations are the default indexes of them used in the BO code. We set npf=50 and nps=50 by default. For example, since npf+nps*(s-1)+4 is the s -th perturbed density, which means $50+50*(2-1)+4=104$ is the default index of the perturbed density for the 2nd species.

1. electric field in x -direction (V/m)	δE_x	2. electric field in y -direction (V/m)	δE_y
3. electric field in z -direction (V/m)	δE_z	4. magnetic field in x -direction (T)	δB_x
5. magnetic field in y -direction (T)	δB_y	6. magnetic field in z -direction (T)	δB_z
7. electric field energy density (J/m^3)	δU_E	8. Magnetic field energy density (J/m^3)	δU_B
9. fraction of field energy in the electric field	$\frac{\delta U_E}{(\delta U_E + \delta U_B)}$	10. fraction of electric field energy in δE_x	$\frac{ \delta E_x ^2}{ \delta E ^2}$
11. fraction of electric field energy in δE_y	$\frac{ \delta E_y ^2}{ \delta E ^2}$	12. fraction of electric field energy in δE_z	$\frac{ \delta E_z ^2}{ \delta E ^2}$
13. a measure of how electrostatic is	$\frac{ k \cdot \delta E ^2}{(k^2 \delta E ^2)}$	14. another measure of how electrostatic is	$\frac{ k \cdot \delta E ^2}{ k \cdot \delta E ^2 + k \times \delta E ^2}$
15. fraction of magnetic field energy in δB_x	$\frac{ \delta B_x ^2}{ \delta B ^2}$	16. fraction of magnetic field energy in δB_y	$\frac{ \delta B_y ^2}{ \delta B ^2}$
17. fraction of magnetic field energy in δB_z	$\frac{ \delta B_z ^2}{ \delta B ^2}$	18. magnetic polarization ellipticity	ϵ_B
19. angle of major axis of magnetic ellipse	θ_B	20. magnetic polarization ratio, $ \alpha_B $	$\frac{ \delta B_y }{ \delta B_x }$
21. angle of magnetic polarization ratio, ϕ_B	$\arg\left(\frac{\delta B_y}{\delta B_x}\right)$	22. wave group velocity in x -direction (m/s)	v_{gx}
23. wave group velocity in z -direction (m/s)	v_{gz}	24. spatial growth rate in x -direction, S_x	$\frac{\omega_i}{v_{gx}}$
25. spatial growth rate in z -direction (m^{-1}), S_z	$\frac{\omega_i}{v_{gz}}$	26. total spatial growth rate (m^{-1}), S	$\frac{\omega_i}{ v_g }$
27. refractive index	$ n $	28 to 36. dispersion tensor elements $i, j = 1, 2, 3$	D_{ij}
...
npf-6. current density in x -direction (A/m^2)	δJ_x	npf-5. current density in y -direction (A/m^2)	δJ_y
npf-4. current density in z -direction (A/m^2)	δJ_z	npf-3. perpendicular wave vector (m^{-1})	k_x
npf-2. parallel wave vector (m^{-1})	k_z	npf-1. wave vector (m^{-1})	k
npf. wave frequency (s^{-1})	ω	npf+nps*(s-1)+1. s -th perturbed x -current (A/m^2)	δJ_{sx}
npf+nps*(s-1)+2. s -th perturbed y -current (A/m^2)	δJ_{sy}	npf+nps*(s-1)+3. s -th perturbed z -current (A/m^2)	δJ_{sz}
npf+nps*(s-1)+4. s -th perturbed density (m^{-3})	δn_s	npf+nps*(s-1)+5. s -th perturbed x -velocity (m/s)	δv_{sx}
npf+nps*(s-1)+6. s -th perturbed z -velocity (m/s)	δv_{sz}	npf+nps*(s-1)+7. s -th perturbed z -velocity (m/s)	δv_{sz}
npf+nps*(s-1)+8. s -th species compressibility	$\frac{ \delta n_s / n_{s0} ^2}{ \delta B / B_0 ^2}$	npf+nps*(s-1)+9. s -th species Alfvén-ratio	$\frac{ \delta v_s / v_A ^2}{ \delta B / B_0 ^2}$
npf+nps*(s-1)+10. s -th parallel phase ratio	$\frac{\text{Re}[\delta n_s \cdot \delta B_z^*]}{ \delta n_s \delta B_z }$	npf+nps*(s-1)+11. s -th kinetic energy fraction x	$\frac{ \delta v_{sx} ^2}{ \delta v_s ^2}$
npf+nps*(s-1)+12. s -th kinetic energy fraction y	$\frac{ \delta v_{sy} ^2}{ \delta v_s ^2}$	npf+nps*(s-1)+13. s -th kinetic energy fraction z	$\frac{ \delta v_{sz} ^2}{ \delta v_s ^2}$
npf+nps*(s-1)+14. s -th kinetic energy fraction k	$\frac{ k \cdot \delta v_s ^2}{ k ^2 \delta v_s ^2}$	npf+nps*(s-1)+15. s -th perturbed velocity magnitude	$ \delta v_s $
npf+nps*(s-1)+16. s -th kinetic energy	δU_{Ks}	npf+nps*(s-1)+17. s -th kinetic energy fraction	$\frac{\delta U_{Ks}}{\delta U_{tot}}$
npf+nps*(s-1)+18:26. s -th conductivity tensor elements	$\sigma_{s,ij}$
...

The linear polarizations can have arbitrary large magnitude. After we obtain the eigenvectors $\delta X_0 = [\delta E_{x0}, \delta E_{y0}, \delta E_{z0}, \delta B_{x0}, \dots]$ in the code, the normalization of modes is done like this

$$\delta X_1 = \frac{\delta X_0}{\delta E_{x0}}, \quad \delta X = \frac{\delta X_1}{|\delta E_{x1}|^2 + |\delta E_{y1}|^2 + |\delta E_{z1}|^2}, \quad (\text{B.1})$$

which causes δE_x to be real and positive, and $|\delta E| = \sqrt{|\delta E_x|^2 + |\delta E_y|^2 + |\delta E_z|^2} = 1$ V/m. This procedure will work except for some extreme cases for which $|\delta E_x| < 10^{-16} |\delta E|$ in double precision calculations. Equations to calculate

some other relevant field quantities are

$$|\delta E_x|^2 = \delta E_x \cdot \delta E_x^* = [Re(\delta E_x)]^2 + [Im(\delta E_x)]^2, \quad \text{similar for } |\delta E_y|^2, |\delta E_z|^2, |\delta B_x|^2, |\delta B_y|^2, |\delta B_z|^2 \quad (\text{B.2})$$

$$|\delta \mathbf{E}|^2 = |\delta E|^2 = |\delta E_x|^2 + |\delta E_y|^2 + |\delta E_z|^2, \quad \delta U_E = \frac{1}{2} \cdot \frac{1}{2} \epsilon_0 |\delta E|^2, \quad (\text{B.3})$$

$$|\delta \mathbf{B}|^2 = |\delta B|^2 = |\delta B_x|^2 + |\delta B_y|^2 + |\delta B_z|^2, \quad \delta U_B = \frac{1}{2} \cdot \frac{1}{2} \frac{|\delta B|^2}{\mu_0}, \quad (\text{B.4})$$

$$|\mathbf{k} \cdot \delta \mathbf{E}|^2 = |k_x \cdot \delta E_x + k_z \cdot \delta E_z|^2, \quad (\text{B.5})$$

$$|\mathbf{k} \times \delta \mathbf{E}|^2 = |-k_z \cdot \delta E_y|^2 + |k_z \cdot \delta E_x - k_x \cdot \delta E_z|^2 + |k_x \cdot \delta E_y|^2, \quad (\text{B.6})$$

where the asterisk denotes complex conjugation. The extra $\frac{1}{2}$ in δU_E and δU_B is for a time average. Note that usually $|\delta E_{x,y,z}|^2 \neq \delta E_{x,y,z}^2$, because $|\delta E_{x,y,z}|^2$ is always real, whereas $\delta E_{x,y,z}^2$ is usually complex. The total energy density $\delta U_{tot} = \delta U_E + \delta U_B + \delta U_K$, where

$$\delta U_K = \sum_s \delta U_{Ks}, \quad \delta U_{Ks} = \frac{1}{2} \cdot \frac{1}{2} m_s n_{s0} |\delta v_s|^2 + \frac{1}{2} \cdot \frac{1}{2} m_s (v_{dsx}^2 + v_{dsy}^2 + v_{dsz}^2) |\delta n_s|. \quad (\text{B.7})$$

To get the magnetic ellipticity, we use

$$\alpha_B \equiv \frac{\delta B_y}{\delta B_x} = |\alpha_B| e^{i\phi_B}, \quad \text{with } |\alpha_B| = \left| \frac{\delta B_y}{\delta B_x} \right|, \quad \phi_B \equiv \arg \left(\frac{\delta B_y}{\delta B_x} \right), \quad (\text{B.8})$$

$$\delta B_L = \delta B_x + i\delta B_y, \quad \delta B_R = \delta B_x - i\delta B_y, \quad \epsilon_B = \frac{|\delta B_R| - |\delta B_L|}{|\delta B_R| + |\delta B_L|}. \quad (\text{B.9})$$

If $\epsilon_B = 1$, the wave is right hand circularly polarized, if $\epsilon_B = 0$, the wave is linearly polarized, and if $\epsilon_B = -1$, the wave is left-hand circularly polarized.

The quantity θ_B is the angle of major axis of the magnetic ellipse, and it should satisfy

$$\theta_B = \tan^{-1} \left[\frac{|\alpha_B| \cos(\phi_B + \varphi)}{\cos \varphi} \right], \quad (\text{B.10})$$

where φ is the angle for the following quantity be at maximum

$$f(\varphi) = \cos^2 \varphi + |\alpha_B|^2 \cos^2(\phi_B + \varphi), \quad (\text{B.11})$$

i.e., its derivative vanishes

$$\frac{\partial}{\partial \varphi} [\cos^2 \varphi + |\alpha_B|^2 \cos^2(\phi_B + \varphi)] = -2 \sin(2\varphi) - 2|\alpha_B|^2 \sin[2(\phi_B + \varphi)] = 0, \quad (\text{B.12})$$

$$\frac{\partial^2}{\partial \varphi^2} [\cos^2 \varphi + |\alpha_B|^2 \cos^2(\phi_B + \varphi)] = -4 \cos(2\varphi) - 4|\alpha_B|^2 \cos[2(\phi_B + \varphi)] < 0, \quad (\text{B.13})$$

which yields

$$\varphi = \frac{1}{2} \cot^{-1} \left[-\frac{(1/|\alpha_B|^2) + \cos(2\phi_B)}{\sin(2\phi_B)} \right], \quad \text{and required } \cos(2\varphi) + |\alpha_B|^2 \cos[2(\phi_B + \varphi)] > 0. \quad (\text{B.14})$$

If $\cos(2\varphi) + |\alpha_B|^2 \cos[2(\phi_B + \varphi)] < 0$, we set $\varphi \rightarrow \varphi + \frac{\pi}{2}$ since the difference between major axis and minor axis is $\frac{\pi}{2}$. Using above equations, we can obtain $|\alpha_B|$, ϕ_B and θ_B . If $\phi_B = \pi/2$ or $\in (0, \pi)$, the wave is left-hand polarization; if $\phi_B = -\pi/2$ or $\in (-\pi, 0)$, the wave is right-hand polarization; if $\phi_B \simeq 0$, or $|\alpha_B| \gg 1$ or $\ll 1$, the wave is linear polarization; if $|\alpha_B| = 1$, the wave is circular polarization; other case, the wave is elliptical polarization.

The species compressibility, parallel phase ratio and Alfvén-ratio are calculated using definitions in Refs.[7, 8]. The refractive index $n = \frac{ck}{\omega}$. The phase velocity $v_p = \frac{\omega}{k}$, the group velocity $v_g = \frac{\partial \omega}{\partial k}$. For $F(\omega, \mathbf{k}) = 0$, using the implicit function derivative formula, we have $v_g = \frac{\partial \omega}{\partial k} = -\frac{\partial F / \partial k}{\partial F / \partial \omega}$, where $F(\omega, \mathbf{k}) = |\mathbf{M}(\mathbf{k}) - \omega|$ or $F(\omega, \mathbf{k}) = |D(\omega, \mathbf{k})|$. However, calculating this is very complicated. Thus, we can use numerical differentiation to calculate the group velocity; i.e., after we obtain a ω for a given (k_x, k_z) , we solve the dispersion relation with $(k_x + \Delta k_x, k_z)$ and $(k_x, k_z + \Delta k_z)$, which gives $\omega + \Delta \omega_x$ and $\omega + \Delta \omega_z$. The group velocity is then $v_{gx} = \frac{\Delta \omega_x}{\Delta k_x}$ and $v_{gz} = \frac{\Delta \omega_z}{\Delta k_z}$.

Appendix C. Typos or bugs fixed in BO 1.0

In BO version 1.0[1], some typos are found. In page 352, $T_{zs} = \frac{1}{2}k_B m_s v_{zts}^2$ and $T_{\perp s\sigma} = \frac{1}{2}k_B m_s v_{\perp ts\sigma}^2$ should be $k_B T_{zs} = \frac{1}{2}m_s v_{zts}^2$ and $k_B T_{\perp s\sigma} = \frac{1}{2}m_s v_{\perp ts\sigma}^2$.

In page 360,

$$\bullet P_{s32}^m = \sum_{n=-\infty}^{\infty} \int_{-\infty}^{\infty} \int_0^{\infty} \frac{2\pi v_{\perp}' dv_{\perp}' dv_{\parallel}''}{(\omega_{sn} - k_z v_{\parallel}'')} \Pi_{s\sigma 32} = \sum_{n=-\infty}^{\infty} \left\{ [n\omega_{cs} \frac{A_{nbs\sigma}}{v_{\perp ts\sigma}^2} \frac{Z_1}{k_z} + A_{n0\sigma} \frac{k_z v_{zts} Z_2}{v_{zts}^2}] v_{d_{sy}} + [n\omega_{cs} \frac{A_{nbs\sigma}}{v_{\perp ts\sigma}^2} \frac{Z_0}{k_z v_{zts}} + A_{n0\sigma} \frac{Z_1}{v_{zts}^2}] v_{d_{sy}} v_{d_{sz}} + i[(n\omega_{cs} - iv_s) \frac{B_{nbs\sigma}}{v_{\perp ts\sigma}} \frac{Z_1}{k_z} + B_{n0\sigma} \frac{v_{\perp ts\sigma} Z_2}{v_{zts}}] + iv_{d_{sz}} [(n\omega_{cs} - iv_s) \frac{B_{nbs\sigma}}{v_{\perp ts\sigma}} \frac{Z_0}{k_z v_{zts}} + B_{n0\sigma} \frac{v_{\perp ts\sigma} Z_1}{v_{zts}^2}] \right\}.$$

should be

$$\bullet P_{s32}^m = \sum_{n=-\infty}^{\infty} \int_{-\infty}^{\infty} \int_0^{\infty} \frac{2\pi v_{\perp}' dv_{\perp}' dv_{\parallel}''}{(\omega_{sn} - k_z v_{\parallel}'')} \Pi_{s\sigma 32} = \sum_{n=-\infty}^{\infty} \left\{ [n\omega_{cs} \frac{A_{nbs\sigma}}{v_{\perp ts\sigma}^2} \frac{Z_1}{k_z} + A_{n0\sigma} \frac{v_{zts} Z_2}{v_{zts}^2}] v_{d_{sy}} + [n\omega_{cs} \frac{A_{nbs\sigma}}{v_{\perp ts\sigma}^2} \frac{Z_0}{k_z v_{zts}} + A_{n0\sigma} \frac{Z_1}{v_{zts}^2}] v_{d_{sy}} v_{d_{sz}} + i[(n\omega_{cs} - iv_s) \frac{B_{nbs\sigma}}{v_{\perp ts\sigma}} \frac{Z_1}{k_z} + B_{n0\sigma} \frac{v_{\perp ts\sigma} Z_2}{v_{zts}}] + iv_{d_{sz}} [(n\omega_{cs} - iv_s) \frac{B_{nbs\sigma}}{v_{\perp ts\sigma}} \frac{Z_0}{k_z v_{zts}} + B_{n0\sigma} \frac{v_{\perp ts\sigma} Z_1}{v_{zts}^2}] \right\}.$$

where the k_z in the numerator of $v_{d_{sy}}$ term should be removed, i.e., $k_z v_{zts} Z_2$ should be $v_{zts} Z_2$. Otherwise, the dimension/unit is incorrect. The terms $v_{\perp}' \Pi_{s\sigma 32}$ in page 360 and P_{s32}^m in page 364 should also be updated accordingly. This will affect the final matrix in the code for $v_{d_{sy}} \neq 0$ cases.

References

- [1] H.S. Xie, BO: A unified tool for plasma waves and instabilities analysis, *Comput. Phys. Comm.* 244 (2019) 343-371.
- [2] H.S. Xie, Y. Xiao, PDRK: A General Kinetic Dispersion Relation Solver for Magnetized Plasma, *Plasma Sci. Technol.* 18 (2) (2016) 97, <http://dx.doi.org/10.1088/1009-0630/18/2/01>, Update/bugs fixed at <http://hsxie.me/codes/pdrk/> or <https://github.com/hsxie/pdrk/>.
- [3] H. S. Xie, PDRF: A general dispersion relation solver for magnetized multi-fluid plasma, *Comput. Phys. Comm.* 185 (2014) 670-675.
- [4] H. Sun, J. Zhao, H. Xie, and D. Wu, On Kinetic Instabilities Driven By Ion Temperature Anisotropy and Differential Flow in the Solar Wind, *The Astrophysical Journal*. 884 (2019) 44.
- [5] H. Sun, J. Zhao, W. Liu, H. Xie, and D. Wu, Electron Temperature Anisotropy and Electron Beam Constraints from Electron Kinetic Instabilities in the Solar Wind, *The Astrophysical Journal*. 902 (2020) 59.
- [6] K. Ronnmark, WHAMP - Waves in Homogeneous Anisotropic Multicomponent Magnetized Plasma, KGI Report No. 179, Sweden, 1982.
- [7] S. P. Gary, The mirror and ion cyclotron anisotropy instabilities, *Journal of Geophysical Research: Space Physics*, 1992, 97, 8519-8529.
- [8] R. E. Denton, M. R. Lessard, J. W. LaBelle and S. P. Gary, Identification of low-frequency magnetosheath waves, *Journal of Geophysical Research: Space Physics*, 1998, 103, 23661-23676.
- [9] L. N. Hau and B. U. Sonnerup, On slow-mode waves in an anisotropic plasma, *Geophysical Research Letters*, 1993, 20, 1763-1766.
- [10] G. F. Chew, M. L. Goldberger and F. E. Low, The Boltzmann Equation and the One-Fluid Hydromagnetic Equations in the Absence of Particle Collisions, *Proceedings of the Royal Society of London. Series A, Mathematical and Physical Sciences*, The Royal Society, 1956, 236, pp. 112-118.